Sequence-Dependent Interactions of Two Forms of UvrC with DNA Helix-Stabilizing CC-1065−N3-Adenine Adducts†

Michael Nazimiec,‡ Chong-Soon Lee,§ Yen-Len Tang,|| Xiancang Ye,‡ Roger Case,‡ and Moon-shong Tang*,‡,⊥

University of Texas M. D. Anderson Cancer Center, Science Park, Smithville, Texas 78957, Department of Biochemistry, College of Science, Yeungnam University, Kyongsan, Korea, Department of Biophysics, Johns Hopkins University, Baltimore, Maryland 21218, and Department of Environmental Medicine, New York University School of Medicine, Tuxedo, New York 10987

Received May 9, 2001; Revised Manuscript Received July 16, 2001

ABSTRACT: The *uvrA*, *uvrB*, and *uvrC* genes of *Escherichia coli* control the initial steps of nucleotide excision repair. The *uvrC* gene product is involved in at least one of the dual incisions produced by the UvrABC complex. Using single-stranded (ss) DNA affinity chromatography, we have separated two forms of UvrC from both wild-type *E. coli* cells and overproducing cells. UvrCI elutes at 0.4 M KCl, and UvrCII elutes at 0.6 M KCl. In general, both forms, in the presence of UvrA and UvrB, actively incise UV-irradiated and CC-1065-modified DNA in the same fashion; i.e., they incise six to eight nucleotides 5′ to and three to five nucleotides 3′ to a photoproduct or a CC-1065−N3-adenine adduct. They produce different incisions, however, at a CC-1065−N3-adenine adduct in the sequence 5′-GATTA*CG- present in the *Msp*I−*Bst*NI 117 bp fragment of M13mp1. UvrABCI incises at both the 5′ and 3′ sides of the adduct (UvrABCI cut), while UvrABCII incises only at the 5′ side (UvrABCII cut). Mixing UvrCI and UvrCII results in both UvrABCI and UvrABCII cuts, and the levels of these two types of cutting are proportional to the amount of UvrCI and UvrCII. DNase I footprints of the *Msp*I−*Bst*NI 117 bp DNA fragment containing a site-directed CC-1065−adenine adduct at the 5′-GATTA*CG- site show that UvrCII, but not UvrCI, binds to the adduct site. Furthermore, the pattern of DNase I footprints induced by UvrCII binding differs from the pattern of the footprints induced by UvrA, UvrAB, and UvrABCI binding. Interestingly, while the presence of unirradiated DNA enhances the efficiency of UvrABCII in incising UV-irradiated DNA, it does not enhance UvrABCII incision of the CC-1065−N3-adenine adduct formed at 5′-GATTA*CG-. These results show that two different forms of UvrC differ in DNA binding properties as well as incision modes at some kinds of DNA damage.

The *uvrA*, *uvrB*, and *uvrC* genes of *Escherichia coli* control the initial steps of excision repair of DNA damaged by ultraviolet (UV)[1] radiation and chemical carcinogens which destabilize the DNA helical structure (for reviews, see refs *1*−*4*). We have found that Uvr proteins are also able to incise DNA damage introduced by DNA helix-stabilizing chemicals, such as anthramycin, mitomycin C, and CC-1065 (*5*−*8*). In general, the purified *uvrA*, *uvrB*, and *uvrC* gene products act in concert to incise both 5′ (six to eight bases) and 3′ (three to five bases) to the damaged bases(s) (*9*). However, incision on only the 5′ or 3′ side of a particular adduct also occurs concomitantly with dual incisions. Single incisions have been reported at pyrimidine dimers, *N*-(deoxyguanosin-8-yl)-2-acetylaminofluorene, *N*-(deoxyguanosin-8-yl)-2-aminofluorene, psoralen, anthramycin, and CC-1065 DNA adducts (*5*, *7*, *10*−*13*).

The mechanism which determines whether a single or dual incision is made by the UvrABC nuclease is unclear, although there are several plausible models. (1) Single 3′ incision events have been produced by using aged UvrC or suboptimal reaction conditions (*14*). (2) The mode of UvrABC incision may be dependent on the conformation of the damaged DNA (which may in turn depend on the particular DNA sequence) (*12*). (3) There may be multiple forms of the enzyme which incise the same damaged DNA differently.

In most of the reported cases, single incision represents an uncommon minority of the incision events. We have reported previously an instance when a single 5′ incision was the predominant product of the UvrABC reaction. We have found that the UvrABC complex preferentially incises on the 5′ side of the CC-1065-modified adenine in the sequence 5′-GATTA*CG- present in the 117 bp *Msp*I−*Bst*NI fragment from M13mp1 (*7*).

We have recently separated UvrC into two forms. One form elutes at 0.4 M KCl (UvrCI), while the other elutes at

† This research was supported by Grants ES03124 and ES08389 from the U.S. Public Health Service.

* To whom correspondence should be addressed: Department of Environmental Medicine, New York University School of Medicine, Tuxedo, NY 10987. E-mail: tang@env.med.nyu.edu. Telephone: (845) 731-3585. Fax: (845) 351-2385.

‡ University of Texas M. D. Anderson Cancer Center.

§ Yeungnam University.

|| Johns Hopkins University.

⊥ New York University School of Medicine.

[1] Abbreviations: ss, single-stranded; ds, double-stranded; UV, ultraviolet; EDTA, ethylenediaminetetraacetic acid; SDS, sodium dodecyl sulfate; PAGE, polyacrylamide gel electrophoresis; DTT, dithiothreitol; RF, replicative form; dTTP, thymidine triphosphate.

10.1021/bi010953p CCC: $20.00
Published on Web 08/22/2001

0.6 M KCl (UvrCII) from ss-DNA cellulose (*15*). In the presence of UvrA and UvrB, these two forms of UvrC incise the CC-1065-modified adenine in the 5′-GATTA*CG- sequence differently (for convenience, we have termed the collective functions of UvrA and UvrB with UvrCI and UvrCII as UvrABCI and UvrABCII, respectively); UvrABCI incises 3′ as well as 5′ to the damaged base, while UvrABCII incises principally on the 5′ side. In addition, UvrABCI recognizes the other modified sites in the 117 bp fragment more efficiently. We have found that while UvrCII binds to the CC-1065−N3-adenine adduct at the 5′-GATTA*CG- site, UvrCI does not, and the pattern of DNase I footprints induced by UvrCII differs from that induced by UvrA and the $(UvrA)_2UvrB$ complex. The possible mechanisms for these sequence-dependent incisions on the CC-1065−N3-adenine adduct by UvrABCI and UvrABCII are discussed.

MATERIALS AND METHODS

Materials. Restriction enzymes *Msp*I, *Sal*I, and *Hin*fI, T4 polynucleotide kinase, bacterial alkaline phosphatase, acrylamide, bisacrylamide, agarose, and NACS Prepacs convertible columns (NACS PACS) were obtained from Bethesda Research Laboratories. The restriction enzyme *Bst*NI was obtained from DuPont New England Biolabs. Yeast tRNA was obtained from Sigma Chemical Co. All ^{32}P-labeled nucleotides were obtained from Amersham Co. or DuPont New England Nuclear.

Purification of UvrCI and UvrCII. UvrC is present in wild-type *E. coli* at only low levels (ca. 20 molecules/cell), thereby necessitating its purification from cells harboring overproducing plasmids. Two suitable plasmid constructions have been described (*16*, *17*). The plasmid pDR3274, carried in CH296 (*uvrC34*) or DR1984 (*recA1*, *uvrC34*) cells, which contains the complete *uvrC* structural gene under the control of an inducible *tac* promoter, was a generous gift of A. Sancar (University of North Carolina at Chapel Hill, Chapel Hill, NC). UvrC was purified from CH296/pDR3274 cells after induction with 1.0 mM isopropyl β-D-thiogalactoside for 18 h. Cells were harvested, washed in 0.3 M sucrose and buffer A [50 mM Tris-HCl (pH 7.5), 1.0 mM EDTA, and 0.1 mM DTT], suspended in $^1/_{20}$ volume of 0.3 M KCl and buffer A, and sonicated for minimal times on ice (30 s bursts at a 50% duty cycle for a total of 1.5−2 min with a microprobe), with cell breakage monitored by absorbance at a wavelength of 600 nm (A_{600}). After centrifugation (20000*g* for 60 min), the supernatant was either applied directly to a phosphocellulose column equilibrated with 0.3 M KCl and buffer A or precipitated with polymin, resuspended in 0.3 M KCl and buffer A, and then applied to the phosphocellulose column, after which chromatography was employed by eluting with buffer A containing KCl gradients ranging from 0.3 to 1 M. A peak of UvrC was located near 0.5 M KCl by SDS gel electrophoresis and corresponded to the major peak of A_{280}-absorbing material. UvrC-containing fractions were combined, diluted to 0.3 M KCl using 0.2 M KCl and buffer A (dialyzed vs 50 volumes of 0.3 M KCl and buffer A for 2 h in some preparations), and applied to a fresh column of ss-DNA cellulose equilibrated with 0.3 M KCl and buffer A. The ss-DNA cellulose column was developed with a continuous gradient of 0.3 to 1.0 M KCl. In this preparation, two-thirds of the UvrC eluted in a peak at 0.4 M KCl, and one-third of the protein eluted in a peak at 0.6 M KCl (*15*). The two forms are designated UvrCI and UvrCII, respectively. This preparation avoids any protein precipitation and may be completed within 12 h of cell lysis. By purification of just the peak material of the phosphocellulose column on ss-DNA cellulose, UvrC containing no SDS−PAGE detectable impurities was prepared (*15*). However, to ensure that no significant portion of the protein preparation was excluded, we have performed several purifications in which a range of fractions encompassing the phosphocellulose peak was subjected to ss-DNA cellulose chromatography. We found that the KCl concentration must be maintained at 0.2 M during the purification to avoid precipitation of the overproduced protein. Results similar to those described above were obtained by substituting 0.1 mM DTT for the 10 mM β-mercaptoethanol in the buffers and even in the absence of added reducing agent. The enzyme prepared in the presence of DTT and 50% glycerol is very stable, and no loss of activity was detected after storage for 1 year at −70 °C.

The UvrCI and UvrCII proteins have the same apparent molecular weight after SDS−PAGE of 65000 as previously reported for UvrC (*16*, *17*). UvrC purified with or without polymin precipitation reacted identically in the experiments reported here.

End Labeling DNA Fragments with ^{32}P. (1) 3′ End ^{32}P Labeling MspI−BstNI 117 bp and Other DNA Fragments from M13mp1 and pBR322. M13mp1 RF DNA (19 μg, 4 pmol) was reacted in a total volume of 10 μL with 20 units of *Bst*NI (10 units/μL) in the supplier's buffer containing 0.2 mg/mL bovine serum albumin for 30 min at 60 °C. The reaction was quenched on ice, and the 3′ termini of DNA fragments were labeled at room temperature by the addition of 8 μL of [α-^{32}P]dTTP (10 μCi/μL) and DNA polymerase I (Klenow fragment) in a total volume of 20 μL. The fragments were purified by phenol/chloroform extraction, centrifugation through G-50 in 10 mM Tris-HCl (pH 7.5) and 10 mM EDTA, phenol/chloroform extraction, chloroform extraction, and ethanol precipitation in the presence of 1 M ammonium acetate. Typical recoveries were 2×10^7 cpm (Cherenkov counting). This treatment generated three singly 3′-end-^{32}P-labeled *Bst*NI fragments [1809 bp (positions 6401−1014), 952 bp (positions 1014−1996), and 127 bp (positions 6274−6401)] and a 137 bp fragment in which both 3′ ends were ^{32}P labeled. These DNA fragments were separated on a 5% acrylamide gel and recovered by electroelution. The 137 bp fragment was further reacted with 50 units of *Msp*I to generate a single 3′-end-^{32}P-labeled 117 bp *Msp*I−*Bst*NI fragment, and this fragment was purified on a 5% acrylamide gel, electroeluted, phenol extracted as described above, and ethanol precipitated. The above preparation also supplies the 127 bp *Bst*NI−*Bst*NI fragment as a singly 3′-end-labeled DNA. The *Eco*RI−*Bst*NI 129 bp fragments of pBR322 were 3′ end labeled with ^{32}P as described previously (*12*).

(2) 5′ End ^{32}P Labeling the MspI−BstNI 117 bp DNA Fragment from M13mp1. The 250 bp fragments isolated from *Msp*I digestion of M13mp1 RF DNA were 5′ end ^{32}P labeled with sequential bacterial alkaline phosphatase and T4 polynucleotide kinase treatment and then digested with *Bst*NI to generate the singly 5′-end-^{32}P-labeled *Msp*I−*Bst*NI 117 bp fragments as described previously (*7*). The *Eco*RI−*Hae*III

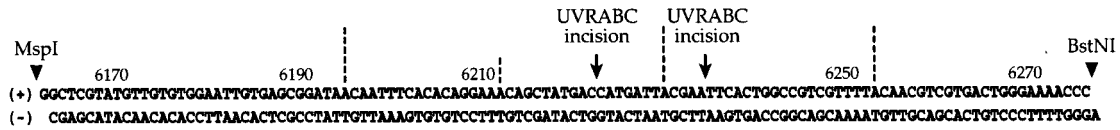

FIGURE 1: DNA sequences of the *Msp*I−*Bst*NI 117 bp fragment of M13mp1 RF DNA. The CC-1065 binding sites are indicated by dotted lines, and the length of the lines represents the relative affinity of drug binding. The UvrABC incision sites for the CC-1065−adenine adduct at the GATTACG site are denoted with arrows. The numerical system is the same as in M13mp1.

174 and 78 bp fragments of pBR322 were 5′ end labeled with ^{32}P as described previously (*12*).

CC-1065 Modification. CC-1065 was dissolved in dimethylformamide and stored at −20 °C at a concentration of 280 μM ($\epsilon_{365} = 48$ mM^{-1}). Dilutions of this solution were made into TE buffer [10 mM Tris (pH 7.5) and 1 mM EDTA] just prior to use. Mixtures of labeled DNA and CC-1065 with final concentrations of 1.4×10^{-3} to 1.4×10^{-1} μM CC-1065 and 10000−100000 cpm of ^{32}P-end-labeled DNA (estimated specific activity of 10^6 cpm/μg) were reacted at 37 °C for 2 h. The modified DNA was precipitated with 2 volumes of −20 °C ethanol after the addition of ammonium acetate (final concentration of 2.5 M) and washed with 70% ethanol. The precipitation was repeated, and the DNA was dissolved in TE buffer.

*Construction of the MspI−BstNI 117 bp DNA Fragment and the 73-mer Containing a Site-Directed CC-1065−Adenine Adduct at the 5′-GATTA*CG- Site.* Construction of the *Msp*I−*Bst*NI 117 bp fragments containing a CC-1065−N3-adenine adduct at the 5′-GATTA*CG- site was the same as described previously (*7*). To construct the 73-mer with a CC-1065−N3-adenine adduct at the 5′-GATTA*CG- site, two synthetic oligonucleotides (5′-TCGTCCAGGTTCGGAAACAGCTGTGACCATGATTACGGATTCACTGG- and 5′-TCGAGCGTCGACGAATTCGCCGACGGCCAGTGAATCCGTAATCATGGTC-) were hybridized to form a DNA duplex and reacted with CC-1065, and the single-strand regions in the DNA duplex were filled by DNA polymerase I to form a double-stranded 73-mer. Subsequently, the 73-mers were digested with *Sal*I and 3′ end labeled with ^{32}P as described above. This 73-mer contains only one CC-1065 binding site at 5′-GATTA*CG-.

UV Irradiation. ^{32}P-labeled DNA fragments were irradiated with a germicidal lamp (Sylvania, C15T8, major emission at 254 nm) to produce one cyclobutane pyrimidine dimer per DNA molecule, as previously described (*18*).

UvrABC Nuclease Reactions. UvrA and UvrB proteins were purified from *E. coli* K12 strain CH296 carrying plasmids pUNC45 (*uvrA*) and pUNC211 (*uvrB*). Purifications were essentially as described by Sancar and Rupp (*9*) with some modifications (*19*). The plasmids and strain CH296 were kindly provided by A. Sancar. An aliquot of modified labeled DNA (usually 10000 cpm for a final DNA concentration of 0.6−2.0 nM) was reacted in 50 mM Tris-HCl (pH 7.5), 10 mM $MgCl_2$, 100 mM KCl, 1 mM ATP, and 1 mM DTT. UvrA, UvrB, and UvrC proteins were added, giving a final concentration of 15 nM each or as indicated in a final volume of 25 μL. Reaction times were as indicated at 37 °C. Reactions were terminated by phenol/chloroform/isoamyl alcohol (1:0.96:0.04) extractions followed by chloroform extractions. The DNA was then precipitated in the presence of ammonium acetate (1 M) with 2.5 volumes of ethanol, washed with 80% ethanol, dried, and dissolved in 80% formamide, 10 mM NaOH tracking dye mix (0.1% xylene cyanol and 0.1% bromophenol blue).

DNase I Footprinting of the Binding of the CC-1065−Adenine Adduct by Uvr Proteins. The *Msp*I−*Bst*NI 117 bp DNA fragments containing a site-directed CC-1065−adenine adduct at the 5′-GATTA*CG- site were 5′ end labeled with ^{32}P at the non-drug-binding strand and reacted with Uvr proteins as in the UvrABC nuclease reaction described above. The method of DNase I footprinting on the Uvr−DNA complexes is the same as that described previously (*7*).

Denaturing Gel Electrophoresis. Chemical sequencing was carried out as described by Maxam and Gilbert (*20*) with the modifications described previously (*12*). UvrABC reaction products were applied to a sequencing gel, consisting of 8% acrylamide and 7 M urea in TBE buffer [50 mM Tris-HCl, 50 mM sodium borate, and 10 mM EDTA (pH 8.3)], in parallel with the Maxam and Gilbert sequencing reactions (*20*). After electrophoresis, the gel was dried in a Bio-Rad gel dryer and exposed to Kodak X-Omat RP film at −70 °C for various lengths of time. The intensity of the bands was determined by scanning with a Bio-Image Analyzer.

RESULTS

UvrCI and UvrCII Can Be Differentiated by Characteristic Incisions at CC-1065−DNA Adducts. CC-1065 is an antitumor antibiotic from *Streptomyces zelensis* which reacts with adenine in ds-DNA in a sequence-dependent manner (*21*). In contrast to bulky chemical carcinogen-induced DNA adducts which cause destabilization of the DNA helix, CC-1065−DNA adducts stabilize the helix; this was evident by the increase in the melting temperature and resistance to S1 nuclease digestion of CC-1065-modified DNA (*22*). The CC-1065−DNA adducts are also heat labile; heating the modified DNA leads to strand breakage at the adducted position, which can be visualized on DNA sequencing gels (*23*, *24*). Previously, using UvrC proteins eluting at 0.65 M KCl from ss-DNA cellulose chromatography, we found that these UvrC proteins, working together with UvrA and UvrB, incise only at the 5′ side of the CC-1065−N3-adenine adduct formed at the 5′-GATTA*CG- sequence in the *Msp*I−*Bst*NI 117 bp fragment of M13mp1 (Figure 1), and that these Uvr proteins do not incise CC-1065−DNA adducts formed at the other three CC-1065 binding sites [TTTTA*-, -GATAA*-, and -GGAAA*- (*7*)]. We have recently separated the UvrC proteins into two forms and discovered that the two forms of UvrC have different affinities for ds-DNA binding (*15*). We then further tested the reaction of these two forms of UvrC toward the CC-1065−DNA adducts formed in this *Msp*I−*Bst*NI 117 bp fragment. The 117 bp fragments singly 3′ end labeled at the *Bst*NI site were modified with moderate (0.02−0.2 μM) CC-1065 concentrations, followed by reactions with UvrCI and UvrCII in the presence of UvrA and UvrB, and the resulting DNA was separated by denaturing

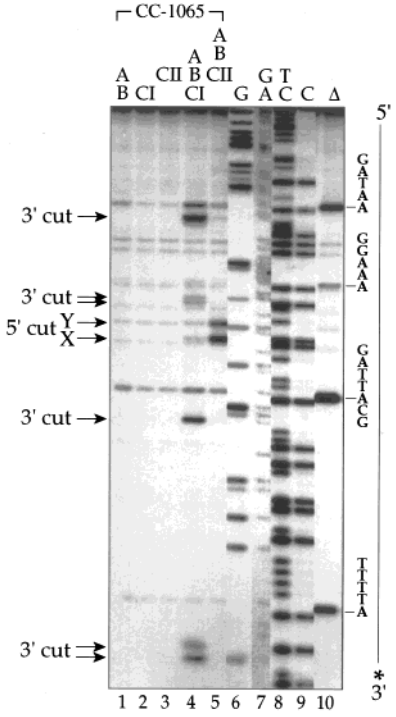

FIGURE 2: UvrABCI and UvrABCII incisions of the CC-1065-modified 3′-end-^{32}P-labeled *Msp*I−*Bst*NI 117 bp fragment of M13mp1 RF DNA. DNA fragments were purified, 3′ end labeled with ^{32}P, modified with CC-1065 (lanes 1−5 and 10), and then reacted with UvrA and UvrB (lane 1), UvrCI (lane 2), UvrCII (lane 3), UvrABCI (lane 4), UvrABCII (lane 5) or heated at 90 °C for 10 min (lane 10) as described in the text. The resultant DNAs were separated by electrophoresis in an 8% denaturing polyacrylamide gel. Lanes 6−9 are the G, GA, TC, and C reactions, respectively (*20*). AB, CI, CII, ABCI, and ABCII represent DNA reacted with UvrA and UvrB, UvrCI, UvrCII, UvrABCI, and UvrABCII, respectively. The CC-1065−DNA adduct-induced thermal alkaline labile bands (lane 10 at the -TTTTA*-, -GATTA*-, -GGAAA*-, and -GATAA*- sequences, where A* represents the CC-1065 binding adenine) are indicated at the right, and the UvrABCI-cut and UvrABCII-cut bands are indicated at the left. Y and X represent DNA fragments with and without CC-1065 binding, respectively, resulting from UvrABCII cuts at the -GATTA*CG- sequence. The polarity and the labeled end (*) of the ^{32}P-labeled DNA strand are indicated at the right side of the panel.

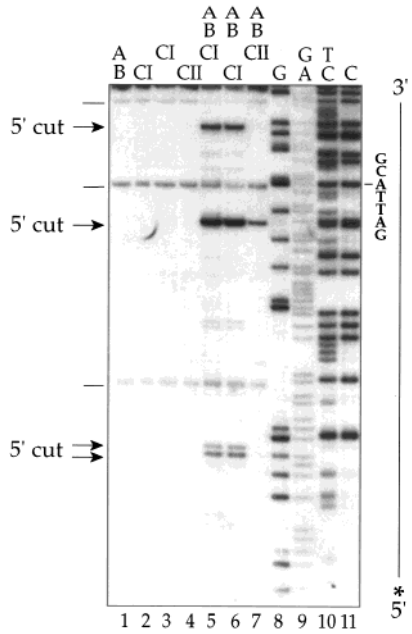

FIGURE 3: UvrABCI and UvrABCII incisions of the CC-1065-modified 5′-end-^{32}P-labeled *Msp*I−*Bst*NI 117 bp fragment of M13mp1RF DNA. DNA fragments were purified, 5′ end labeled with ^{32}P, modified with CC-1065 (lanes 1−7), and then reacted with UvrA and UvrB (lane 1), UvrCI (lanes 2 and 3), UvrCII (lane 4), UvrABCI (lanes 5 and 6), or UvrABCII (lane 7) as described in the text. The resultant DNAs were separated by electrophoresis in an 8% denaturing polyacrylamide gel. Lanes 8−11 are the G, GA, TC, and C reactions, respectively (*18*). The CC-1065−DNA adduct-induced thermal-alkaline labile bands (—) and the UvrABCI-cut and UvrABCII-cut bands (arrows) are indicated at the left. The -GATTACG- sequence is indicated at the right. The polarity and the labeled end (*) of the ^{32}P-labeled DNA strand are indicated at the right side of the panel.

gel electrophoresis. The results in Figure 2 show that UvrABCII incisions are primarily 7 bp 5′ to the CC-1065−DNA adduct formed at the sequence 5′-GATTA*CG- (A* denotes the adduct formation site, which is at position 6229 in M13mp1) and that the other adduct sites are poorly recognized, if at all (Figure 2, lane 5). These results are similar to the results we previously reported for this DNA fragment (*7*). UvrABCI, in contrast, produces an incision 3′ to the CC-1065−DNA adduct formed at the 5′-GATTA*CG- site (Figure 2, lane 4). Furthermore, Figure 2 shows that UvrABCI recognized all four of the CC-1065 adducts (-TTTTA*-, -GGAAA*-, and -GATAA*-) identified by heat treatment in the test substrate (Figure 2, lane 10). At each adduct position, UvrABCI incisions were found 3 or 4 bp 3′ to the adduct site. We note that signals significantly lower than the 3′ incision bands are found 5′ to the -GATTA*CG- site on the 3′-end-labeled DNA fragment; these results suggest that the UvrCI preparation contains some UvrCII. Incisions by UvrABCI at three different modification levels are similar, and their extents appear to be proportional to the modification level as determined by heat treatment.

The appearance of a DNA fragment of a length corresponding to the incisions 5′ to the adducted adenine on a 3′-labeled DNA can only mean that the corresponding 3′ incision was not made by the enzyme. The 5′ incisions found on this 3′-labeled DNA lie in two bands (X and Y in lane 5, Figure 2) located 7 and 11 bp 5′ to the -GATTA*CG- adduct site. The first (X band) of these bands (7 bp 5′ to the adduct) probably represents DNA which has undergone incision as well as loss of the CC-1065 molecule. We conclude that the Y band represents 5′-incised DNA fragments which retain CC-1065. The Y band, according to Maxam−Gilbert sequencing lanes, appears in a position between the bases located 11 and 12 bp from the adduct at the -GATTA*CG- site, which is consistent with a conformational rather than length origin for the size difference. The intensity of the autoradiographic bands located 11 bp 5′ to the adduct was greatly diminished by longer (10−30 min) heating times at 90 °C prior to loading the reaction products on the gel (data no shown). A 2 min, 90 °C heat treatment was adopted in the standard assay to minimize thermal incisions of 5′-UvrABC-incised DNA at the -GATTA*CG- site, which could lead to an underestimation of the 5′ incision level.

The results in Figure 3 show UvrABCI and UvrABCII reactions with CC-1065-modified 5′-end-labeled *Msp*I−*Bst*NI 117 bp DNA. The 5′ incision produced by UvrABCI at the -GATTA*CG- site occurred 7 bp 5′ to the modification, as expected. At the other two CC-1065 modification sites, UvrABCI produces 5′ incisions 7 or 8 bp 5′ to the modification site (Figure 3, lanes 5 and 6). UvrABCII

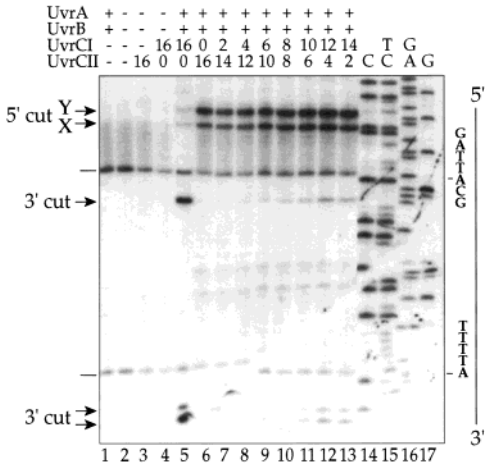

FIGURE 4: Effect of UvrCI and UvrCII on UvrABC incision of the CC-1065-modified 3′-end-^{32}P-labeled *Msp*I−*Bst*NI 117 bp fragment of M13mp1 RF DNA. CC-1065-modified DNA fragments (lanes 1−13) were reacted with different ratios of UvrCI and UvrCII (total concentration of 16 nM) in the presence of 15 nM UvrA or 15 nM UvrB under the standard UvrABC reaction conditions as described in the text. Only the CC-1065−DNA adduct-induced thermal alkaline labile bands (—) and the UvrABCI-cut and UvrABCII-cut bands (arrows) at the -GATTA*CG- and -TTTTA*- sites are shown. The numbers at the top of the panel represent the concentrations (in nanomolar) of UvrC added, and the symbols + and − represent with and without Uvr proteins, respectively. X and Y represent the same DNA fragments as described in the legend of Figure 2. The polarity and the labeled end (*) of the ^{32}P-labeled DNA strand are indicated at the right side of the panel.

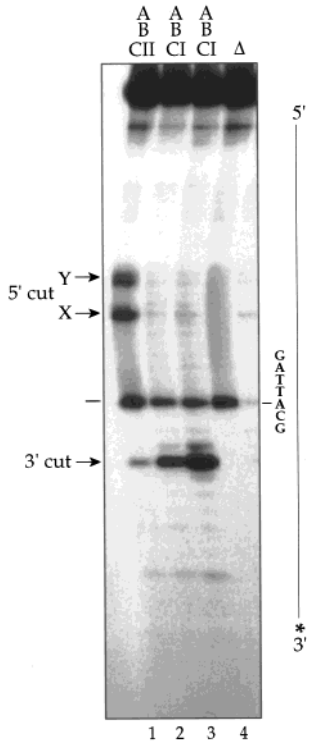

FIGURE 5: UvrABCI and UvrABCII incisions of the CC-1065-modified 3′-end-^{32}P-labeled synthetic 73-mer. Double-stranded 73-mers were constructed, 3′ end labeled with ^{32}P, modified with CC-1065 (lanes 1−4), and then reacted with UvrABCI (lanes 2 and 3) or UvrABCII (lane 1) or heated at 90 °C for 5 min (lane 4) as described in the text. The resultant DNAs were separated by electrophoresis in an 8% denaturing polyacrylamide gel. The CC-1065−DNA adduct-induced thermal alkaline labile band (lines, —) at the -GATTA*CG- site and the UvrABCI-cut and UvrABCII-cut bands (arrows) are indicated. X and Y represent the same DNA fragments as described in the legend of Figure 2. The polarity and the labeled end (*) of the ^{32}P-labeled DNA strand are indicated at the right side of the panel.

produces a 5′ incision 7 bp to the CC-1065 adduct at the -GATTA*CG- site on 5′-end-labeled 117 bp DNA, with no evidence of a 3′ incision. These results are consistent with UvrABCII making only 5′ incisions at this site. As with 3′-end-labeled DNA, the other modification sites on the 5′-end-labeled DNA are incised poorly, if at all, by UvrABCII (Figure 3, lane 7).

Adding both UvrCI and UvrCII in the reaction including UvrA and UvrB and the 3′-end-labeled 117 bp modified with CC-1065 resulted in both UvrABCI and UvrABCII cuts (Figure 4, lanes 7−13). In this experiment, the intensities of the incision bands resulting from pure UvrCI (lane 5), UvrCII (lane 6), and a series of different proportions of UvrCI and UvrCII are compared. Two results are evident from the series of reactions in lanes 7−13. (1) The uncoupled incision at the 5′ side of the -GATTA*CG- sequence, a characteristic of UvrABCII, predominates as the UvrCII concentration increases, showing that UvrCII activity may mask UvrCI activity. (2) Both UvrCI and UvrCII may be active in the same reaction, and the UvrABCI cutting intensity is proportional to the UvrCI concentration in the mixture. The latter effect is more evident in the cutting at the 5′-TTTTA*- site shown in the bottom of the gel.

UvrABCI and UvrABCII Produce the Same Characteristic Incisions on a CC-1065-Modified Synthetic Oligomer. The distinct incision pattern of UvrABCI and UvrABCII on the CC-1065−adenine adduct at the -GATTA*CG- site in the 117 bp fragment could be due to reaction of UvrABCI and UvrABCII with different populations of the DNA fragments carrying different extents of CC-1065 modification and/or with different sites of CC-1065 modification. To test this possibility, we have used two chemically synthesized oligonucleotides to construct a 73 bp fragment which contains a -GATTA*CG- site and its surrounding 37 bp sequences that are identical to the 117 bp fragment but has no other CC-1065 binding site. These DNA fragments were 3′ end labeled with ^{32}P on the drug-binding strand, modified with 1.4×10^{-2} μM CC-1065, and then reacted with UvrABCI or UvrABCII. The results in Figure 5 show that UvrABCI incisions were found primarily 4 bp 3′ to the CC-1065 adduct at the -GATTA*CG- site in a position identical to that found in the longer 117 bp fragment (Figure 5, lanes 2 and 3). UvrABCII incisions were again found 7 and 11 bp 5′ to the CC-1065-modified adenine (Figure 5, lane 1). These results are identical to the results obtained by using CC-1065-modified 117 bp fragments, and indicate that the uncoupled 5′ incision on the CC-1065−adenine adduct at the -GATTA*CG- site by UvrABCII reflects the unique structure of the drug−DNA adduct at this sequence as well as an intrinsic property of UvrABCII.

UvrABCI and UvrABCII Similarly Incise CC-1065-Modified Adenines on Other DNA Fragments. To investigate the sequence effect on the incision of CC-1065−N3-adenine adducts by UvrABCI and UvrABCII, we have further determined the incision patterns by these two enzyme complexes on six more DNA fragments modified with CC-1065. These fragments were either 5′ or 3′ end labeled with ^{32}P, and the sites of CC-1065 modification were identified

Table 1: UvrABCI and UvrABCII Incisions at CC-1065-Modified Adenines in Different DNA Sequences

sequence origin	size (bp)	CC-1065-modified sequence	labeling end	incisions[a] (bases from modified site) UvrABCI 5′	UvrABCI 3′	UvrABCII 5′	UvrABCII 3′
M13mp1							
*Msp*I−*Bst*NI (6159−6274)	117	GATTA*CG	3′	−	4	7	−
		GATAA*CA	3′	−	4	−	4
		GGAAA*CA	3′	−	4	−	−
		GTTTA*CA	3′	−	4	−	−
*Bst*NI−*Bst*NI (1014−1966)	952	ACTAA*AC	3′	−	4	−	−
		ACTTA*TA	3′	−	4, 5	−	−
*Bst*NI−*Bst*NI (6401−1014)	1809	TATTA*AC	3′	−	4	−	4
		AATGATTA*AA	3′	−	4	−	4
		AATTA*AA	3′	−	4, 5	−	4, 5
		ATTA*CT	3′	−	4, 5	−	4, 5
		ATTTA*CT	3′	−	4, 5	−	4, 5
		CAAGATTA*CT	3′	−	4, 5	−	4, 5
*Bst*NI−*Bst*NI (6274−6401)	127	TAATA*GC	3′	−	4, 5	−	4, 5
pBR322							
*Eco*RI−*Bst*NI (4359−130)	129	TTAAA*TT	3′	−	5	−	5
*Eco*RI−*Hae*III (4359−173)	174	TTAAA*TT	5′	7	−	−	−
*Hae*III−*Bam*HI (296−375)	79	AAGTA*CG	5′	7	−	−	−
		CGATA*GT	5′	7	−	8	−
M13mp1						7	
*Msp*I−*Bst*NI (6159−6274)	117	GATTA*CG	5′	7	−	7	−
synthetic	73	GATTA*CG	3′	−	4	7	−

[a] The symbol − denotes that cutting was not observed.

by alkaline heat treatment. The results in Table 1 show that the patterns of UvrABCI and UvrABCII incision of the CC-1065−N3-adenine adducts are identical for 16 different sequences, including a 5′-GATTA*CT- sequence and a 5′-GATTA*AA- sequence. These results suggest the unique feature which leads to the unusual 5′ side only UvrABCII cut is dependent on not only the 5′ side sequence of the target adenine but also its 3′ site sequence. At present, we have not yet determined precisely the crucial sequences at the 3′ side of the adenine adduct which will determine the UvrABCII specificity.

Incision of UV-Induced Photoproducts in the MspI−BstNI 117 bp Fragment of M13mp1. Since no significant difference in the incision of CC-1065−DNA adducts by UvrABCI and UvrABCII was observed in DNA fragments other than the *Msp*I−*Bst*NI 117 bp fragment of M13mp1, these results suggest that this particular DNA fragment may have unusual structure. It is therefore of interest to determine whether these two forms of UvrC proteins have qualitative or quantitative differences in incising UV-induced photoproducts in this fragment. The 3′-^{32}P-end-labeled 117 bp fragments were UV irradiated to produce one photodimer per fragment followed by reaction with UvrABCI or UvrABCII (Figure 6). The efficiency of incision of the UV photoproducts by UvrABCII is much lower than that by UvrABCI at most photoproduct sites; however, there are significant differences in the incision pattern between these two enzyme complexes. The photodimer formed at the 5′-GAT<>TACG- (T<>T represents the cyclobutane thymine dimer) site is refractory to UvrABCII but is sensitive to UvrABCI, and the cuts by the latter render a two-band pattern (the cuts occur either 3 or 4 nucleotides 3′ to the photodimer). Photodimers formed at the other sequences are sensitive to both UvrABCI and UvrABCII; however, the cuts by the former are significantly stronger than those by the latter. Band M in lane 2 could result from a UvrABCII incision 3 nucleotides 3′ to the photodimer formed at the -AC<>TGG- site or an incision 7 nucleotides 5′ to the photodimer formed at -GTCGTT<>TT-.

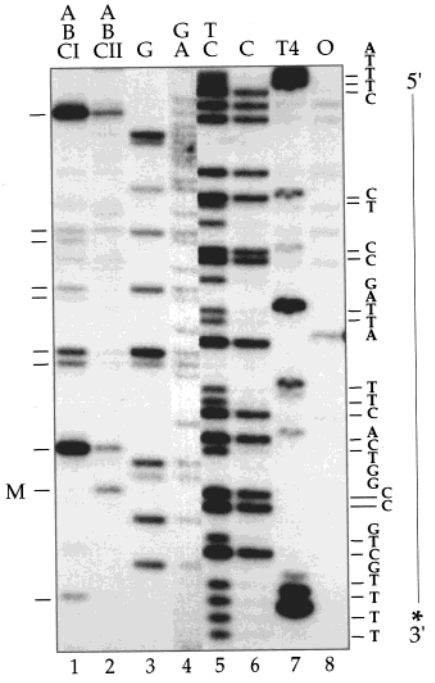

FIGURE 6: UvrABCI and UvrABCII incisions of UV-irradiated 3′-end-^{32}P-labeled *Msp*I−*Bst*NI 117 bp fragments of M13mp1 RF DNA. DNA fragments were purified, 3′ end labeled with ^{32}P, irradiated with UV to produce one cyclobutane pyrimidine dimer per DNA fragment, and then reacted with UvrABCI (lane 1) or UvrABCII (lane 2) as described in the legend of Figure 2, or with T4 endonuclease V (lane 7). Lane 8 is the control DNA. Lanes 3−6 are Maxam and Gilbert G, GA, TC, and C reactions, respectively. Sequences of interest (-GATTA-, -ACTGG-, and -GTCGT-) are indicated at the right side of the panel. Lines at the right represent contiguous pyrimidines, and lines at the left represent the UV photoproduct-induced UvrABCI- and UvrABCII-cut bands. The polarity and the labeled end (*) of the ^{32}P-labeled DNA strand are indicated at the right side of the panel.

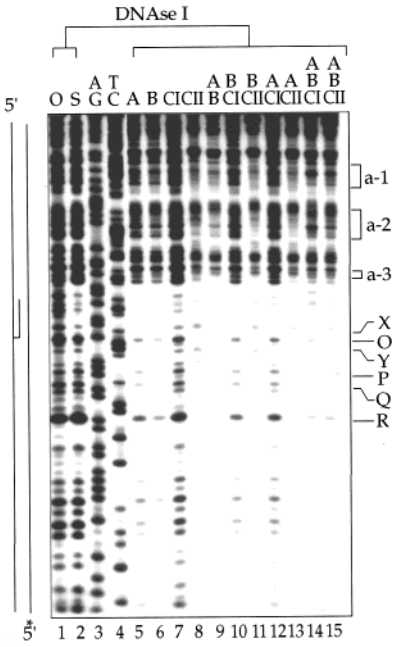

FIGURE 7: DNase I footprints on the Uvr-bound *Msp*I−*Bst*NI 117 bp fragment of M13mp1 containing a site-directed CC-1065−adenine adduct at the 5′-GATTA*CG- site. The non-drug-binding strand of the *Msp*I−*Bst*NI 117 bp fragment was 5′ end labeled with ^{32}P, and the DNA fragments were then reacted with Uvr proteins individually or in different combinations under standard UvrABC reaction conditions. At the end of the incubation, DNase I was added as described in the text (lanes 1, 2, and 5−15). The resultant DNA was then separated by electrophoresis in an 8% polyacrylamide gel as described in the legend of Figure 2. Lanes 3 and 4 are purine and pyrimidine reactions, respectively (*23*). Lanes 1 and 2 are DNA without and with a site-directed CC-1065 adduct, respectively, reacted with DNase I directly, and lanes 5−15 are DNA with a site-directed CC-1065 adduct treated with Uvr proteins as indicated (A represents UvrA, B UvrB, CI UvrCI, etc.) and then treated with DNase I as described in the text. The Uvr−CC-1065 adduct binding induced DNase I footprinting areas (a-1, a-2, and a-3) and bands (X, O, Y, P, Q, and R) are indicated. The polarity, the ^{32}P-labeled end (*), and the CC-1065 binding site are indicated at the left side of the panel.

*Binding of UvrCII but Not UvrCI to the CC-1065−Adenine Adduct at the 5′-GATTA*CG- Sequence.* Since UvrABCII and UvrABCI incise the CC-1065−adenine adduct at the 5′-GATTA*CG- sequence differently from adducts at other sequences, it is of interest to examine the interaction between Uvr proteins and the drug−DNA adduct at this particular sequence. An *Msp*I−*Bst*NI 117 bp fragment containing a site-directed CC-1065−adenine adduct at the 5′-GATTA*CG- site was constructed, and the non-drug-binding strand was 5′ labeled with ^{32}P as described previously (*7*, *25*). These DNA fragments were reacted with Uvr proteins individually or in combination under standard UvrABC reaction conditions, and were subsequently digested with DNase I to determine the level of Uvr protein binding. The results in Figure 7 show that UvrCII as well as UvrA and UvrB binds to the drug−DNA adducts while UvrCI does not bind (lanes 5−8). Although it appears that these Uvr proteins bind more to the 3′ side of the CC-1065 binding site than to the 5′ side region, UvrCII binding causes changes in the footprinting pattern at the 5′ side region (brackets a-1, a-2, and a-3) which are not observed with the UvrA and UvrB binding (lanes 5, 6, and 8). Furthermore, the patterns of binding of UvrCII with UvrA and/or UvrB are similar to those of UvrCII alone, but are different from those of UvrA, UvrB, UvrAB, and UvrABCI. For example, X and Y bands observed in DNAs that bind to UvrCII with UvrA and/or UvrB (lanes 8, 11, 13, and 15) are much stronger than those that bind with UvrA, UvrB, UvrAB, and UvrABCI (lanes 5, 6, 9, and 14). There are significant changes in the footprinting of UvrA, UvrAB, and UvrABCI (see bands O−R), and the changes are not the same as those that have been found in DNA fragments containing site-directed cyclobutane dipyrimidines or psoralen (*26*−*28*), where UvrA binding induces 33 bp footprints and binding of UvrAB reduces the footprinting to 19 bp. It is worth noting that footprints 8 bases beyond 5′ upstream and 6 bases beyond 3′ downstream of the drug binding site become similar for UvrABCI and UvrABCII binding; however, within this region, there are distinct differences.

*Effects of Competitive DNA on the UvrABCI and UVRABCII Incisions of the CC-1065−N3-Adenine Adduct at the -GATTA*CG- Site.* We have found that UvrCII is a ds-DNA binding protein while UvrCI is not, and this UvrCII−DNA binding may interfere with proper $(UvrA)_2UvrB$ photoproduct complex formation and consequently inhibit the dual incisions of the photoproduct by the UvrABC complex; furthermore, we have found that the affinity of binding of UV-irradiated DNA by UvrA is higher than that by UvrCII (*15*). These UvrCII−DNA binding-induced inhibitory effects on UvrABC incision of the photoproduct, however, can be eliminated by adding nondamaged competitive DNA (*15*). In contrast, the results in Figure 7 show that UvrA does not significantly affect the DNase I footprints of the binding of the CC-1065−N3-adenine adduct at the -GATTA*CG- site by UvrCII. These results suggest that the binding affinity of the CC-1065−adenine adduct at the -GATTA*CG- site by UvrCII may be stronger than that of UvrA under these reaction conditions. If this is the case, then we expect that competitive DNA may have different effects on the UvrABCII incision of photoproducts and the CC-1065−adenine adduct at the -GATTA*CG- site. To test this possibility, we have reacted UvrABCII with the CC-1065-modified and UV-irradiated *Msp*I−*Bst*NI 117 bp fragment of M13mp1 in the presence of different amounts of competitive DNA. The results in Figure 8A shows that the presence of competetive DNA reduces the intensity of the UvrABCII incision on the CC-1065−DNA adduct without increasing the intensity of the characteristic UvrABCI incision. In constrast, while the presence of competitive DNA enhances UvrABCII incision at the phtodimer formed at the -ATTT<>C-, −AAT<>TCA-, and -GTT<>TT- sites, it reduces the level of cutting of the photodimer formed at the -AC<>TGG- site (compare lane 1 to 3 in Figure 8B).

DISCUSSION

We have purified two forms of UvrC proteins from overproducing cells and have demonstrated that these two forms of UvrC also exist in wild-type *E. coli* cells (*15*). Although both forms of UvrC, together with UvrA and UvrB, are able to incise photodimers, our results show that UvrCII is a ds-DNA binding protein, but UvrCI is not (*15*). In this paper, we have presented one interesting finding, that is, in the presence of UvrA and UvrB these two forms of UvrC proteins react differently with CC-1065−N3-adenine adducts formed in the *Msp*I−*Bst*NI 117 bp fragment of M13mp,

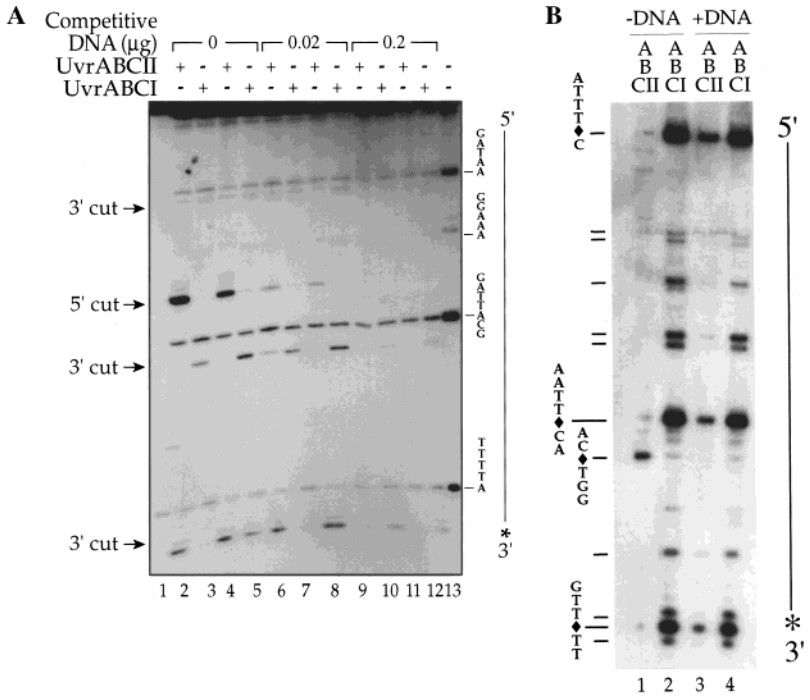

FIGURE 8: Effects of competitive DNA on the UvrABCI and UvrABCII incisions for (A) CC-1065−DNA adducts and (B) UV photoproducts formed in the *Msp*I−*Bst*NI 117 bp fragment of M13mp1 RF DNA. The 3′-end-^{32}P-labeled DNA fragments were either modified with CC-1065 or irradiated with UV as described in the legends of Figures 2 and 6, and then reacted with UvrABCI or UvrABCII in the presence of different amounts of linearized ϕX174 RF DNA: 0 for lanes 1−4 and lane 13, 0.02 μg for lanes 5−8, and 0.2 μg for lanes 9−12 (A) and 0 for lanes 1 and 2 and 0.2 μg for lanes 3 and 4 (B). The resultant DNAs were separated as described in the legend of Figure 2. In panel A, the CC-1065−DNA adduct-induced UvrABCI-cut and UvrABCII-cut bands (−) are indicated at the left side of the panel and the heat-induced CC-1065 adduct bands are indicated by lines (−) at the right side of the panel. In panel B, the photodimer-induced UvrABC-cut bands (−) are indicated at the left side of the panel. The polarity and the labeled end (*) of the ^{32}P-labeled DNA strand are indicated at the right side of the panel. The sequences of interest are indicated, and the symbol <> indicates the photodimer position.

especially with the adduct formed at the 5′-GATTA*CG- site. The reasons why UvrABCII incises only 5′ of the CC-1065−N3-adenine adduct at the 5′-GATTA*CG- site and fails to incise the drug−DNA adduct formed at other sequences in this DNA fragment are unclear. Paradoxically, both UvrABCI and UvrABCII show the same incision patterns for the CC-1065−adenine adduct at 13 other sequences in pBR322 and other M13mp1 fragments (Table 1); these results together strongly suggest that the 5′-GATTA*CG- sequence within the *Msp*I−*Bst*NI 117 bp fragment of M13mp1 RF DNA may have an unusual structure.

Our DNase I footprinting results demonstrate that UvrCII binds strongly to the CC-1065−N3-adenine adduct at the 5′-GATTA*CG- sequence. The footprints of UvrACII and UvrBCII are similar, if not identical, to the footprint of UvrCII alone. In contrast, the footprints of UvrACI and UvrBCI are similar to that of UvrA. These results indicate that the drug−DNA adduct formed at this site may be bound by UvrCII more favorably than by the $(UvrA)_2UvrB$ complex. Consistent with this notion is the finding that competitive DNA has different effects on UvrABCII incisions of the UV-irradiated and CC-1065-modified *Msp*I−*Bst*NI 117 bp fragment of M13mp1 RF DNA (Figure 8).

We observed that addition of UvrB alone also protects the drug-bound DNA from DNAse I digestion. This result indicates that UvrB binds to the CC-1065−adenine adduct at the -GATTACG- site. It has been shown that UvrB does not bind to unmodified double-stranded DNA and the UV photoproduct and psoralen−DNA adduct in ds-DNA (*10*, *26*, *27*); however, recently, it has been found that UvrB binds to ss-DNA (*29*). Our results suggest that the DNA structural changes induced by the CC-1065−adenine adduct at the 5′-GATTA*CG- site may facilitate UvrB binding. What structural changes are required for UvrB−DNA binding and how this UvrB−DNA binding may affect UvrABC incision remain to be determined.

The current understanding of the sequential events of the dual incision by UvrABC for damaged DNA is as follows. The damaged DNA is recognized by the $(UvrA)_2UvrB$ complex either by vector movement of this protein complex or by molecular collision. After binding to the damaged DNA site, UvrA may be released from the complex, and UvrC subsequently joins the $(UvrA)_2UvrB$− or UvrB−DNA damage complex. This binding changes the tertiary structure of UvrB and induces the phosphodiesterase function of UvrB, which incises 3′ of the damaged DNA, and consequently, this 3′ incision further alters the structure of the UvrBC complex to induce the 5′ phosphodiesterase function of the UvrC protein (for a review, see refs *2* and *3*). The lack of a 3′ incision by UvrABCII on the drug−DNA adduct at the -GATTA*CG- sequence demands an alternative mechanism; we propose that at certain sequences UvrCII may bind before the UvrA−UvrB complex, and this UvrCII binding prior to UvrA and UvrB binding may result in a single 5′ side incision rather than in 5′ and 3′ dual incisions. It is quite possible that the same mechanism may exist for some types of damage formed at other sequences; that is, UvrCII may bind to these damaged bases more favorably than the $(UvrA)_2UvrB$ complex does, resulting in a 5′ incision rather than in 5′ and

3′ dual incisions. We have evidence which shows that binding of UvrCII to ds-DNA hinders the formation of the $(UvrA)_2UvrB$ photoproduct complex, and consequently hinders the UvrABC dual incisions of photoproducts (*15*). However, the ds-DNA binding affinity of UvrCII is lower than that of UvrA and can be "diluted out" by addition of "competitive DNA" in the reaction mixture (*15*). We hypothesize that UvrCII may bind to some damaged sites more strongly than UvrA and this binding either prevents formation of the UvrA−UvrB complex or facilitates an unusual UvrCII−UvrABCII complex formation which renders only a 5′ incision.

ACKNOWLEDGMENT

We thank Dr. A. Sancar for providing UvrC-containing plasmids and Dr. Bhanot, G. Iyer, and Y.-Y. Tang for critically reviewing the manuscript.

REFERENCES

1. Friedberg, E. C., Walker, G. C., and Siede, W. (1995) *DNA Repair and Mutatenesis*, ASM Press, Washington, DC.
2. Sancar, A., and Tang, M.-s. (1993) *Photochem. Photobiol. 57*, 905−921.
3. Van Houten, B. (1990) *Photochem. Photobiol. 54*, 18−51.
4. Grossman, L., and Yeung, A. T. (1990) *Mutat. Res. 236*, 213−221.
5. Walter, R. B., Pierce, J., Case, R., and Tang, M.-s. (1988) *J. Mol. Biol. 203*, 939−947.
6. Kohn, H., Li, V.-S., and Tang, M.-s. (1992) *J. Am. Chem. Soc. 14*, 5501−5509.
7. Tang, M.-s., Lee, C.-s., Doisy, R., Ross, L., Needham-VanDevanter, D. R., and Hurley, L. H. (1988) *Biochemistry 27*, 893−901.
8. Tang, M.-s., Nazimiec, M. E., Doisy, R. P., Pierce, J. R., Hurley, L. H., and Alderete, B. E. (1991) *J. Mol. Biol. 220*, 855−866.
9. Sancar, A., and Rupp, W. D. (1983) *Cell 33*, 249−260.
10. Yeung, A. T., Mattes, W. B., Oh, E. Y., Yoakum, G. H., and Grossman, L. (1986) *Nucleic Acids Res. 14*, 8535−8556.
11. Myles, G. M., van Houten, B., and Sancar, A. (1987) *Nucleic Acids Res. 15*, 1227−1243.
12. Pierce, J. R., Case, R., and Tang, M.-s. (1989) *Biochemistry 28*, 5821−5826.
13. Pierce, J. R., Nazimiec, M., and Tang, M.-s. (1993) *Biochemistry 32*, 7069−7078.
14. Selby, C. P., and Sancar, A. (1988) *Biochemistry 27*, 7184−7188.
15. Tang, M.-s., Nazimiec, M. E., Ye, C., Iyer, G. H., Eveleigh, J., Zheng, Y., Zhou, W., and Tang, Y.-Y. (2001) *J. Biol. Chem. 276*, 3904−3910.
16. Thomas, D. C., Levy, M., and Sancar, A. (1985) *J. Biol. Chem. 260*, 9875−9883.
17. Yeung, A. T., Mattes, W. B., Oh, E. Y., and Grossman, L. (1983) *Proc. Natl. Acad. Sci. U.S.A. 80*, 6157−6161.
18. Nazimiec, M., Grossman, L., and Tang, M.-s. (1992) *J. Biol. Chem. 267*, 24716−24724.
19. Tang, M.-s. (1996) Mapping and quantification of bulky chemicals, *Induced DNA damage using UvrABC nuclease* (Pfeifer, G. P., Ed.) pp 137−151, Plenum Press: New York and London.
20. Maxam, A. M., and Gilbert, W. (1980) Sequencing end-labeled DNA with base-specific chemical cleavages, in *Methods in Enzymology* (Grossman, L., and K., M., Eds.) p 65, Academic Press, San Diego.
21. Hurley, L. H., Reynolds, V. L., Swenson, D. H., Petzold, G. L., and Scahill, T. A. (1984) *Science 226*, 843−844.
22. Swenson, D. H., Li, L. H., Hurley, L. H., Rokem, J. S., Petzold, G. L., Dayton, B. C., Wallace, T. L., Lin, A. H., and Krueger, W. C. (1982) *Cancer Res. 42*, 2821−2828.
23. Reynolds, V. L., Molineux, K. J., Kaplan, D. J., Swenson, D. H., and Hurley, L. H. (1985) *Biochemistry 24*, 6228−6237.
24. Tang, M.-s., Qian, M., and Pao, A. (1994) *Biochemistry 33*, 2726−2732.
25. Hurley, L. H., Needham-VanDevanter, D. R., and Lee, C.-S. (1987) *Proc. Natl. Acad. Sci. U.S.A. 84*, 6412−6416.
26. Van Houten, B., Gamper, H., Hearst, J. E., and Sancar, A. (1986) *J. Biol. Chem. 261*, 14135−14141.
27. Van Houten, B., Gamper, H., Hearst, J. E., and Sancar, A. (1988) *J. Biol. Chem. 263* (32), 16553−16560.
28. Bertrand-Burggraf, E., Selby, C. P., Hearst, J. E., and Sancar, A. (1991) *J. Mol. Biol. 219*, 27−36.
29. Hsu, D. S., Kim, S.-T., Sun, Q., and Sancar, A. (1995) *J Biol. Chem. 270*, 8319−8327.

BI010953P